Article:
Qiao, P, Harbottle, D, Tchoukov, P et al. (2 more authors) (2017) Asphaltene Subfractions Responsible for Stabilizing Water-in-Crude Oil Emulsions. Part 3. Effect of Solvent Aromaticity. Energy and Fuels. ISSN 1520-5029

https://doi.org/10.1021/acs.energyfuels.7b01387

Asphaltene Subfractions Responsible for Stabilizing Water-in-Crude Oil Emulsions. Part 3. Effect of Solvent Aromaticity

Peiqi Qiao,† David Harbottle,‡ Plamen Tchoukov,† Xi Wang,† and Zhenghe Xu*,†
†Department of Chemical and Materials Engineering, University of Alberta, Edmonton, Canada
‡School of Chemical and Process Engineering, University of Leeds, Leeds, United Kingdom

ABSTRACT: Whole asphaltenes (WA) were fractionated by the E-SARA method according to their adsorption characteristics at oil−water interfaces from either toluene or heptol solutions. Heptol, a mixture of n-heptane and toluene at a 1:1 volume ratio, is a less aromatic solvent than toluene. The effect of solvent aromaticity on the composition of resulting asphaltene subfractions at oil−water interfaces was studied to determine the key functional groups that are critical to the asphaltene-induced stabilization of water-in-oil (W/O) petroleum emulsions. The interfacially active asphaltenes (IAA) were extracted as materials irreversibly adsorbed onto emulsified water droplets, while the asphaltenes remaining in the oil phase were considered as remaining asphaltenes (RA). Although toluene-extracted interfacially active asphaltenes (T-IAA) accounted for only 1.1 ± 0.3 wt % of WA, this subfraction of asphaltenes exhibited a greater interfacial activity and formed more rigid films at the oil−water interface than IAA extracted using heptol, known as HT-IAA which accounted for 4.2 ± 0.3 wt % of WA. The increased potential of T-IAA to stabilize W/O emulsions was attributed to their higher content of oxygen, resulting in a higher content of sulfoxide groups, as verified by elemental analysis, Fourier transform infrared (FTIR) spectroscopy, and X-ray photoelectron spectroscopy (XPS). Although the toluene-extracted remaining asphaltenes (T-RA) and heptol-extracted remaining asphaltenes (HT-RA) were shown to contain similar H/C ratios and nitrogen contents to those of T-IAA and HT-IAA, the two RA subfractions contained a much less amount of sulfur and oxygen, leading to a much reduced interfacial activity as compared with that of IAA subfractions. In spite of the small proportions in asphaltenes, oxygen-containing functional groups, in particular sulfoxides, were believed to contribute significantly to the increased stability of asphaltene-stabilized W/O petroleum emulsions.

1. INTRODUCTION

Stable water-in-oil (W/O) emulsions are highly undesirable in the petroleum industry since they contribute to the enhanced corrosion of downstream processing equipment and impact production capacity due to difficulties associated with emulsion breaking.[1−3] As such, extensive research efforts have been focused on studying the stabilizing potential of the numerous surface active species native to crude oils, including asphaltenes, naphthenic acids, resins, and fine clays.[2,4] While each component provides some stabilizing potential, overwhelmingly asphaltenes were frequently identified to be a major contributor to stabilizing W/O petroleum emulsions.[1−10] However, it has been shown that not all asphaltenes contribute equally to the stabilization of W/O petroleum emulsions.[2,11] Bitumen washing experiments by Xu et al. showed that less than 2 wt% of Athabasca bitumen was actually responsible for the stabilization of W/O petroleum emulsions.[12] Considering that asphaltenes account for 17−20 wt % of Athabasca bitumen, it is clear that only a small fraction of asphaltenes can be classified as “problematic” and readily stabilize W/O emulsions.[13] Fourier transform ion cyclotron resonance mass spectrometry (FT-ICRMS) was used by Stanford and co-workers[14] to characterize the interfacially active materials extracted from diluted bitumen using the heavy water method proposed by Wu.[15] The asphaltenes irreversibly adsorbed at the oil−water interface were found to contain a higher content of heteroatoms (N, O, and S). Differences in asphaltene chemical composition have also been observed when considering asphaltene deposition onto solid surfaces.[16] Wattana et al. characterized asphaltenes extracted from solid deposits and found that the deposited asphaltenes contained more metals (vanadium, nickel, and iron) and polar fractions than asphaltenes separated from the parent crudes.[17] Differences in chemical composition were also noted by Rogel et al., who reported that asphaltenes extracted from crude oils were less aromatic and more soluble than those present in the deposits.[18] Additional research conducted by Tu et al. confirmed that asphaltenes remaining in solution contained less nitrogen and sulfur than those adsorbed onto clays.[19−21]

It becomes evident that studying fractionated asphaltenes could provide more insights to mitigate asphaltene-related issues, which can be achieved by focusing on the physicochemical properties of asphaltene subfractions that actually cause the problems. Asphaltene precipitation in solvents of low aromaticity has frequently been used to separate asphaltene subfractions.[22−24] Spiecker and co-workers precipitated whole asphaltenes in mixtures of heptane and toluene to obtain two asphaltene subfractions of precipitates and solubles.[22] Compared with the soluble subfraction, the precipitates exhibited a lower H/C ratio and a larger amount of nitrogen, nickel, vanadium, and iron. The stability of W/O emulsions was found to be greatly enhanced by large asphaltene aggregates formed from the precipitate subfraction. Östlund et al. fractionated whole asphaltenes using a mixture of methylene chloride and n-pentane.[23] These authors noted that asphaltenes of lower aromaticity could be precipitated out of solutions by solvents of decreasing methylene chloride to n-pentane ratios, albeit the heteroatom content remained unchanged. While most of

the asphaltene fractionation research to date has considered differences in solubility, it is more informative to fractionate asphaltene molecules according to their adsorption characteristics at oil−water and oil−solid interfaces, which is crucial to providing insights on the most troublesome asphaltene subfractions.

The E-SARA concept proposed by our group describes the fractionation of asphaltenes based on their interfacial activity and adsorption characteristics, providing an effective route to study the physicochemical properties of the most troublesome asphaltene subfractions.[25] Subramanian et al. fractionated asphaltenes based on asphaltene adsorption onto calcium carbonate.[26] The study showed that asphaltenes adsorbed onto calcium carbonate contained a higher amount of carbonyl, carboxylic acid, and/or derivative groups than unadsorbed asphaltenes. Compared with the whole asphaltenes, the asphaltene subfraction deposited on calcium carbonate was shown to preferentially adsorb onto stainless steel surfaces, forming thicker asphaltene layers. By isolating emulsified water droplets, Yang et al. recovered the asphaltene subfraction irreversibly adsorbed at the toluene−water interface, naming it “interfacially active asphaltenes” or IAA.[27] However, the asphaltene subfraction remaining in the bulk oil phase was termed “remaining asphaltenes” or RA. The IAA subfraction was shown to exhibit a higher interfacial activity than the RA subfraction, with the IAA producing thicker and more rigid interfacial films and exhibiting a strong aging effect on interfacial properties and W/O emulsion stability. This research confirmed the notion that only a small subfraction of asphaltenes was responsible for stabilization of W/O petroleum emulsions.

The ability of asphaltenes to stabilize W/O petroleum emulsions is closely related to the self-aggregation of asphaltene molecules, which facilitates the formation of viscoelastic films at oil−water interfaces, thus providing the stabilizing mechanism to inhibit water droplet coalescence.[27−30] Asphaltene aggregation is known to be affected by solvent aromaticity,[6,7,9] with aliphatic solvents promoting the flocculation and precipitation of asphaltenes. Eley et al. reported that the highest stability of W/O emulsions occurred when the solvent conditions approached the asphaltene solubility limit.[31] Using atomic force microscopy (AFM), Wang et al. showed that the interactions between adsorbed asphaltene films in toluene were dominated by steric repulsion.[32] Adding n-heptane significantly reduced the repulsive force, accompanied by an increasing adhesion force. When using a surface forces apparatus (SFA) to study the interactions between asphaltene films deposited on mica in solvents of different aromaticity, Natarajan et al.[33] and Zhang et al.[34] obtained similar results to those of Wang et al. All of these studies highlighted the effect of solvent aromaticity on asphaltene aggregation. It is therefore essential to study the effect of solvent aromaticity on the composition of the IAA subfraction of asphaltenes and physical properties of interfacial asphaltene films in relation to the stability of W/O petroleum emulsions that are of great scientific and practical importance. Following the E-SARA concept, whole asphaltenes (WA) are fractionated into IAA and RA by emulsifying water in asphaltene solutions prepared using solvents of different aromatic contents (toluene and heptol).

Heptol used in this work refers to the mixture of n-heptane and toluene at a 1:1 volume ratio. The composition and molecular structure of asphaltene subfractions have been determined by elemental analysis, Fourier transform infrared (FTIR) spectroscopy, and X-ray photoelectron spectroscopy (XPS), with the chemical structure determined being related to the physical properties of asphaltene subfractions including interfacial tension, interfacial shear rheology, crumpling ratio, and emulsion stability.

2. MATERIALS AND METHODS

2.1. Chemicals. Vacuum distillation feed bitumen from Syncrude Canada, Ltd. (Canada) was used to precipitate WA. Optima-grade toluene, Optima-grade n-heptane, and certified n-pentane (Fisher Scientific, Canada) were used as received. Toluene and n-heptane were chosen as standard solvents, with the aromaticity of the solvent being adjusted by adding an equal volume of n-heptane to toluene (heptol). These solvents represent the boundary of the asphaltene solubility spectra[35] that is commonly encountered in industry. Deionized (DI) water was used throughout the study with a resistivity of 18.2 MΩ·cm was used throughout the study. WA were extracted from bitumen using an excess volume of n-pentane (40:1 by volume) and further washed with n-pentane until the supernatant appeared clear. The fine mineral solids in the resultant asphaltene precipitates were removed by centrifuging the asphaltene-in-toluene solution at 20 000g for 20 min. Further details on asphaltene precipitation can be found in Tchoukov et al.[29]

2.2. E-SARA Fractionation Based on Asphaltene Adsorption at the Oil−Water Interface. WA were fractionated into two subfractions using the method shown in Figure 1. In the toluene-based fractionation, 10 mL of DI water was emulsified in 100 mL of 10 g/L WA-in-toluene solution using a VWR 250 homogenizer (VWR, Canada) operating at 30 000 rpm for 5 min. The W/O emulsion was left undisturbed overnight before centrifuging at 20 000g for 10 min. A brown sediment cake of stable water droplets was separated by carefully removing the supernatant using a transfer pipet. The sediment cake was consecutively washed (6 times) with 40 mL of fresh toluene until the supernatant appeared colorless, confirming the removal of any entrapped asphaltene-in-toluene solution or loosely bound asphaltenes. During each wash, the sediment cake was dispersed by shaking for 5 min and left undisturbed for 1 h prior to removing the supernatant. The supernatants from each wash were collected and combined with the supernatant obtained following

centrifugation. The solvent was evaporated from the supernatants at 60 °C under reduced pressure to obtain asphaltene precipitates, termed toluene-extracted remaining asphaltenes (T-RA). The washed cake was dried in a vacuum oven at 60 °C overnight to evaporate water and toluene. After evaporation, the resulting asphaltene subfraction was collected and termed toluene-extracted interfacially active asphaltenes (T-IAA). Heptol-based fractionation was performed by following the same procedure. WA were fully solubilized in heptol, and visual inspection of the solution confirmed no asphaltene precipitation after centrifugation of the solution at 20 000g for 10 min.[36] The two asphaltene subfractions obtained were termed heptol-extracted interfacially active asphaltenes (HT-IAA) and heptol-extracted remaining asphaltenes (HT-RA). The fractional yields for T-IAA and HT-IAA were 1.1 ± 0.3 wt % and 4.2 ± 0.3 wt %, respectively. All four asphaltene subfractions (T-IAA, T-RA, HT-IAA, and HT-RA) were redissolved in toluene for further analysis, including measurements of interfacial tension, interfacial shear rheology, crumpling ratio, and emulsion stability (bottle test).

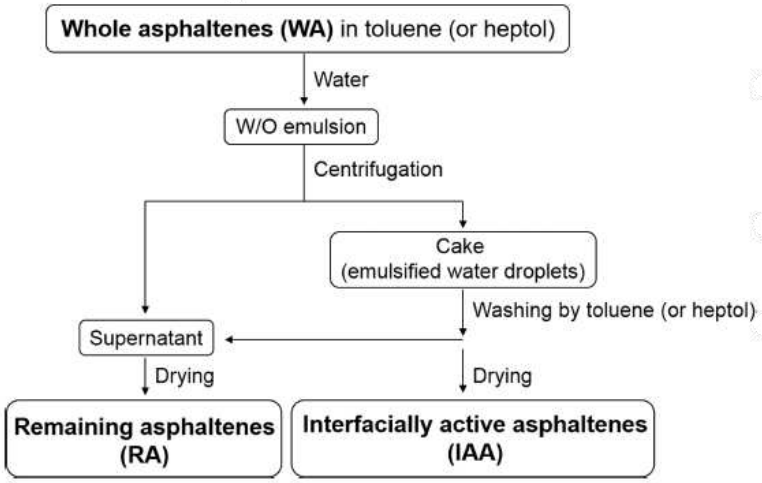

Figure 1. E-SARA fractionation of asphaltenes based on asphaltene adsorption at oil−water interfaces.

2.3. Elemental Analysis. The carbon, hydrogen, nitrogen, sulfur, and oxygen contents of asphaltene subfractions were analyzed using a FLASH 2000 CHNS/O analyzer (Thermo Scientific, U.S.A.). The standard method recommended by the instrument manufacturer was used, in which 5 mg of each asphaltene subfraction was analyzed.

2.4. Fourier Transform Infrared (FTIR) Spectroscopy. FTIR spectra of the asphaltene subfractions were obtained using a Nicolet 8700 FTIR spectrometer (Thermo Scientific, U.S.A.), equipped with a Smart iTR Attenuated Total Reflection (ATR) sampling accessory in the spectral range between 4000 and 800 cm−1, with a spectral resolution of 4 cm−1. A single spectrum was obtained from a total of 128 scans. For semiquantitative analysis, all FTIR spectra obtained were normalized with respect to the absorption band at 2780−3000 cm−1, which is assigned to the aliphatic C−H stretching vibration.

2.5. X-ray Photoelectron Spectroscopy (XPS). XPS analysis of the asphaltene subfractions was performed using a Kratos Axis 165 spectrometer (Kratos, U.K.) under ultrahigh vacuum conditions (the base pressure of the instrument is ∼5 × 10−10 Torr), with a monochromatic Al Kα X-ray source (1486.6 eV) at 15 kV anode potential and 20 mA emission current. The spectrometer was calibrated by the binding energy (84.0 eV) of Au 4f7/2 with reference to the Fermi level. High-resolution scans were performed at a pass energy of 20.0 eV, with a step of 0.1 eV and a dwell time of 200 ms for C 1s, N 1s, S 2p, and O 1s spectra to indicate the distribution of chemical bonds present in asphaltene subfractions. The core-level lines of XPS spectra were fitted using Gaussian and Lorentzian functions by Casa XPS software to determine peak positions, widths, areas, and intensities.

2.6. Interfacial Tension Measurement. The water−oil dynamic interfacial tension was measured using an Attension Theta tensiometer (Biolin Scientific, Finland) at a constant temperature (23 ± 1 °C). A gastight syringe with an inverted 18-gauge needle was used to generate a 20 μL oil droplet (0.1 g/L fractionated asphaltene-in-toluene solution) in a quartz cuvette filled with 10 mL of DI water. Even though the asphaltene concentration in heavy crude oil can greatly exceed the concentration used in the current study,[13] 0.1 g/L asphaltene in solvent was chosen to better elucidate the dynamics of asphaltene adsorption (interfacial tension) and the dynamic nature of asphaltene film formation (interfacial shear rheology). Prior to the measurement, the syringe was first thoroughly rinsed with toluene, acetone, and DI water and then dried using nitrogen. The cuvette was sealed to minimize any solvent loss and atmospheric disturbances

during the measurement. Interfacial tension was recorded at a rate of 5 fps. All experiments were repeated five times to obtain a statistical certainty of a typical experimental error less than 2%.

2.7. Interfacial Shear Rheology. The viscoelasticity of films formed by asphaltene subfractions at toluene−water interfaces was determined using an AR-G2 stress-controlled rheometer (TA Instruments, Canada), equipped with a Pt/Ir double-wall ring (DWR) geometry and a circular Delrin trough. The DWR geometry has a square-edged cross-section, allowing the geometry to "pin" the toluene−water interface. The Delrin trough was placed on a Peliter plate for temperature control. The shear viscoelasticity [storage modulus (G′) and loss modulus (G″)] of asphaltene interfacial films was measured using the harmonic oscillation of the DWR geometry while keeping the interfacial area constant. Details on the measurement technique are given elsewhere.30,37

All shear rheological measurements were conducted at a constant temperature of 23 ± 0.1 °C. Pipetted first into the Delrin trough was 19.2 mL of DI water as the subphase. The DWR geometry was then positioned at the air−water interface, before adding 15 mL of 0.1 g/L fractionated asphaltene-in-toluene solution. Finally, the Delrin trough was covered with a Teflon cap to prevent solvent evaporation and atmospheric disturbances. Aging experiments were performed over 12 h with the measurements at a frequency of 0.5 Hz and 0.5% strain amplitude which were within the linear viscoelastic region, identified by preliminary experiments. Following the aging, frequency sweeps were conducted, in which the frequency was increased from 0.001 to 0.1 Hz at a constant strain amplitude of 0.5%.

2.8. Crumpling Ratio. The mechanical response of the asphaltene stabilized interface was qualitatively evaluated by the crumpling ratio (CR). An oil droplet (0.1 g/L fractionated asphaltene-in-toluene solution) was generated following the procedure outlined in section 2.6 and aged for 1 h in DI water. The oil droplet volume was then slowly decreased at a rate of 20 μL/min, and the crumpling ratio (CR) was determined as CR = Af/Ai, where Af is the projected area of the oil droplet when crumpling is first observed upon contraction, and Ai is the initial projected area of the oil droplet. Sequential droplet images were recorded at 100 fps using an Attension Theta tensiometer (Biolin Scientific, Finland) and analyzed using ImageJ software to determine Af and Ai, and hence the crumpling ratio. All experiments were completed at a constant temperature of 23 ± 1 °C and repeated five times to obtain a statistical certainty of a typical experimental error less than 2%.

2.9. Emulsion Stability by Bottle Test. W/O emulsions were prepared by mixing 10 mL of 0.1 g/L fractionated asphaltene-in-toluene solution and 1 mL of DI water using a VWR 250 homogenizer (VWR, Canada) at 30 000 rpm for 5 min. Optical microscope [Axiovert 200 microscope (Carl Zeiss, Germany)] images of the settled water droplets recovered from the glass vial, 1 cm above the base, were used to determine the droplet size distribution immediately following emulsification and after 1 h of aging. Asphaltene depletion in the bulk oil phase was measured 1 h after emulsification using a Shimadzu UV-3600 spectrophotometer (Shimadzu, U.S.A.). The supernatant absorbance (removed at 1 cm below the air−solution interface) was converted to the concentration using the Beer−Lambert law. The calibration curves for asphaltene subfractions were determined based on the absorbance measured at 409 nm, for fractionated asphaltene-in-toluene solutions in the concentration range between 0.02 g/L and 0.1 g/L.

3. RESULTS

3.1. Elemental Composition and Structure Analysis.

3.1.1. Elemental Analysis. The elemental composition of asphaltene subfractions is summarized in Table 1. HT-RA and T-RA are shown to have similar elemental compositions as anticipated, since both RA subfractions are the dominant species in WA. The fractional yield of HT-IAA is 4.2 ± 0.3 wt%, while the yield of T-IAA is lower at 1.1 ± 0.3 wt %. The H/C ratio varies between 1.16 and 1.20, confirming that all asphaltene subfractions have similar aromaticity. The nitrogen content varies slightly among asphaltene subfractions. However, the two IAA subfractions are quite different from the RA subfractions in terms of sulfur and particularly the oxygen content. Both HT-IAA (9.72 wt % S) and T-IAA (9.78 wt % S) contain higher sulfur content than HT-RA (8.74 wt % S) and T-RA (8.76 wt % S). Furthermore, a significantly higher oxygen content was found in T-IAA (5.62 wt % O), followed by HTIAA (3.71 wt % O), in comparison with lower oxygen contents in T-RA (1.37 wt % O) and HT-RA (1.34 wt % O). Enrichment of oxygen and oxygen−sulfur species in interfacial materials of crude oil has been reported in previous studies.14,38 O2, O4, and O3S classes were found to be enriched in the multilayer asphaltene films stabilizing W/O emulsions at low bitumen concentration in heptol.14 Likewise, in contrast to the less competitive adsorption of N class species, O2 and O4S were found as the two most abundant classes in interfacially active species collected from crude oils of different origins.38

Table 1. Elemental Composition of Asphaltene Subfractions

asphaltene subfraction	element (wt %) C	H	N	S	O	H/C ratio
HT-RA	80.61	8.04	1.11	8.74	1.34	1.20
T-RA	80.67	8.03	1.12	8.76	1.37	1.19
HT-IAA	77.79	7.53	1.13	9.72	3.71	1.16
T-IAA	75.91	7.48	1.12	9.78	5.62	1.18

3.1.2. FTIR Spectroscopy. In general, most of the sulfur bearing functional groups in asphaltenes are thiophenes, sulfides, and sulfoxides, which contain both sulfur and oxygen, while oxygen is present mainly in the forms of hydroxyl, carbonyl, and carboxyl groups.6 FTIR spectroscopy was used to determine the major functional groups contained in asphaltene subfractions. All FTIR spectra were normalized using the strong absorbance peak of the aliphatic C−H stretching vibration in the range of 2780 cm−1 to 3000 cm−1, enabling comparison of the relative amounts of functional groups among the four asphaltene subfractions (Figure 2). The absorbance band observed between 1460 and 1380 cm−1 corresponds to the aliphatic C−H bending vibration, and the band at 1600 cm−1 is assigned to the aromatic C□C stretching vibration. These bands are similar in intensity for all asphaltene subfractions, suggesting the presence of similar hydrocarbon backbones. No noticeable bands were observed for the N−H stretch between 3100 and 3500 cm−1 (not shown in Figure 2), indicating nitrogen atoms are mainly embedded in the aromatic rings for all asphaltene subfractions. The main difference between the spectra of asphaltene subfractions is seen in the spectral range of 1020 cm−1 to 1040 cm−1, which is attributed to the stretching vibration of sulfoxide group. T-IAA appear to exhibit a higher intensity of sulfoxides than HT-IAA, while HT-RA and T-RA show similar but much weaker absorbance, confirming the lower oxygen and sulfur contents of two RA subfractions as revealed also by elemental analysis. The oxygen and sulfur present in IAA subfractions at higher contents, particularly in T-IAA, exist mainly in the form of sulfoxides. The enrichment of sulfoxide groups in the IAA subfractions was also observed in our previous study (see earlier paper in the series),39 although the WA used were from a different source of bitumen. In addition, the C−O bond (C−O stretching at 1100 cm−1) along with hydroxyl (O−H bending at 910 cm−1) and carbonyl (C=O stretching at 1700 cm−1) groups also contribute to the high oxygen content of T-IAA and HT-IAA, but to a lesser extent. Between the two IAA subfractions, T-IAA exhibit a higher amount of oxygen-containing groups than HT-IAA, which is in good agreement with the differences in oxygen content shown by elemental analysis.

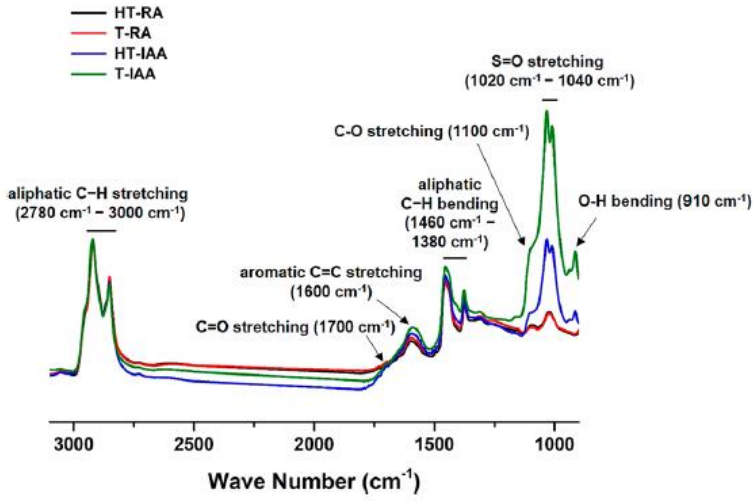

Figure 2. FTIR spectra of asphaltene subfractions.

3.1.3. XPS Analysis. High resolution XPS spectra over C 1s, N 1s, S 2p, and O 1s regions were acquired to investigate the type and the relative proportion of chemical bonds present in asphaltene subfractions (Table 2). The C 1s spectra of asphaltene subfractions were fitted as two peaks with binding energies of 284.8 and 285.8 eV. The main C 1s peak at 284.8 eV represents a systematic carbon bond (C−H or C−C bond), while the subpeak at 285.8 eV is attributed to carbon in a C−O environment.40,41 From Table 2, it is worth noting that among the four asphaltene subfractions, the T-IAA subfraction has the highest relative concentration of C−O bonds, followed by HTIAA,
HT-RA, and T-RA. The

N 1s spectra confirm that nitrogen atoms are present in the forms of pyridinic (398.7 eV) and pyrrolic (400.2 eV) nitrogen[40−43] and in similar concentrations for all asphaltene subfractions. The data are in good agreement with the results from FTIR analysis, which showed nitrogen atoms of asphaltene subfractions to be mainly embedded in the aromatic rings. XPS analysis reconfirms that nitrogen-containing species are not enriched in the different asphaltene subfractions obtained by E-SARA fractionation at oil−water interfaces.

In the S 2p spectra, and 2p3/2 and 2p1/2 components of a single species were fitted with a 2:1 relative intensity and separated in binding energy by 1.2 eV. Two pairs of S 2p peaks were observed in the S 2p spectra of HT-RA and T-RA. The major S 2p3/2 peak was found at a binding energy of 164.0 eV, which corresponds to the presence of thiophenic sulfur,[40−43] while the minor S 2p3/2 peak appearing at 163.2 eV indicates the presence of a small amount of alkyl sulfides.[44,45] However, in the S 2p spectra of HT-IAA and T-IAA, in addition to the two S 2p3/2 peaks at 163.2 and 164.0 eV, a third S 2p3/2 peak was measured at 166.0 eV, which is corresponding to sulfoxides.[42,44,45] Despite the fact that most of the sulfur atoms are present in the form of thiophenes and alkyl sulphides for all asphaltene subfractions, a large amount of sulfur atoms form sulfoxides in IAA subfractions. T-IAA have a higher relative concentration of sulfoxides than HT-IAA, which agrees well with the FTIR results (Figure 2). The absence of this XPS peak in the RA subfractions indicates that the amount of IAA in the RA subfractions is below the detection limit of XPS, typically below 0.5 wt %.

The narrow band O 1s spectra of T-IAA and HT-IAA were deconvoluted, which resulted in two O 1s peaks at 531.5 and 533.0 eV. These peaks are attributed to C=O type and C−O type of oxygen, respectively.[15,40] Based on the studies by Wu,[15] Rudrake et al.,[40] and Abdallah and Taylor,[46] both peaks at binding energies of 532.4 and 533.4 eV in the O 1s spectra of HT-RA and T-RA are attributed to C−O type oxygen in different chemical environments, indicating a negligible amount of C=O bonds in HT-RA and T-RA. These results suggest that IAA subfractions have a greater amount of carbonyl functional groups than RA subfractions, which is consistent with the findings from FTIR analysis.

Table 2. XPS Spectral Features of C 1s, N 1s, S $2p_{3/2}$, and O 1s in Asphaltene Subfractions

element	binding energy (eV)	chemical bond	concentration (%)[a] of chemical bond	element	binding energy (eV)	chemical bond	concentration (%)[a] of chemical bond
		HT-RA				HT-IAA	
C 1s	284.8	C−H or C−C	92.35	C 1s	284.8	C−H or C−C	88.81
	285.8	C−O	7.65		285.8	C−O	11.19
N 1s	398.7	pyridinic	43.96	N 1s	398.7	pyridinic	44.39
	400.2	pyrrolic	56.04		400.2	pyrrolic	55.61
S $2p_{3/2}$	163.2	sulfidic	20.01	S $2p_{3/2}$	163.2	sulfidic	23.26
	164.0	thiophenic	79.99		164.0	thiophenic	57.50
O 1s	532.4	C−O	91.49		166.0	sulfoxide	19.24
	533.4	C−O	8.51	O 1s	531.5	C=O	42.29
					533.0	C−O	57.71
		T-RA				T-IAA	
C 1s	284.8	C−H or C−C	93.58	C 1s	284.8	C−H or C−C	87.13
	285.8	C−O	6.42		285.8	C−O	12.87
N 1s	398.7	pyridinic	43.91	N 1s	398.7	pyridinic	44.28
	400.2	pyrrolic	56.09		400.2	pyrrolic	55.72
S $2p_{3/2}$	163.2	sulfidic	19.55	S $2p_{3/2}$	163.2	sulfidic	23.36
	164.0	thiophenic	80.45		164.0	thiophenic	54.21
O 1s	532.4	C−O	92.13		166.0	sulfoxide	22.43
	533.4	C−O	7.87	O 1s	531.5	C=O	34.01
					533.0	C−O	65.99

[a]The concentration of the element in each chemical state was calculated from the peak area ratio of the element at each specific binding state.

3.2. Interfacial Properties. 3.2.1. Interfacial Tension. The water−oil (0.1 g/L fractionated asphaltene-in-toluene solution) dynamic interfacial tension is shown in Figure 3. For all asphaltene subfractions, the interfacial tension decreases rapidly after droplet production, followed by a slower reduction at longer aging times. Such behavior is often attributed to the diffusion controlled adsorption of asphaltenes, followed by the relaxation and reorganization of the interfacially adsorbed asphaltenes.[47,48] It is not surprising to observe that T-IAA were more interfacially active than HT-IAA, and the least interfacially active subfractions were HT-RA and T-RA. The high interfacial activity of IAA subfractions, notably T-IAA, can be attributed to a significantly higher amount of polar functional groups in IAA subfractions, which exist mainly in the form of sulfoxides. Due to the electronegativity difference between oxygen and sulfur, electron density is drawn from the sulfur atom to the oxygen atom in the S=O bond, making the sulfoxide group a strong hydrogen bond acceptor. The hydrogen bonding of these polar functional groups with water is responsible for the interfacial activity of asphaltene

molecules.39 The T-IAA subfraction has the highest content of sulfoxides along with other oxygen containing functional groups, making it the most interfacially active subfraction. While the sulfoxide content of HT-IAA is lower than that of T-IAA, this asphaltene subfraction contains more sulfoxides than HT-RA and T-RA and thus shows greater interfacial activity. The interfacial tension of WA was studied at an equivalent concentration (0.1 g/L) to T-IAA and HT-IAA, corresponding to 9.1 g/L and 2.4 g/L of WA for T-IAA and HT-IAA, respectively (concentrations determined from the average fractional yields of IAA subfractions, 1.1 wt % for TIAA and 4.2 wt % for HT-IAA). The interfacial tension of WA showed a high degree of similarity to the corresponding data measured using HT-IAA and T-IAA only, confirming the dominating influence of IAA subfractions on the interfacial activity of WA. On the other hand, the interfacial tension of WA at an equivalent concentration (0.1 g/L) to T-RA and HTRA (data not shown) was found to be only slightly (2%) lower than the values measured for the two RA subfractions alone, which could be considered essentially to be within the experimental error. Considering the fact that T-RA accounted for 98.9 ± 0.3 wt % of WA and HT-RA accounted for 95.8 ± 0.3 wt % of WA, this result is not unexpected as the amount of IAA in this case is negligible.

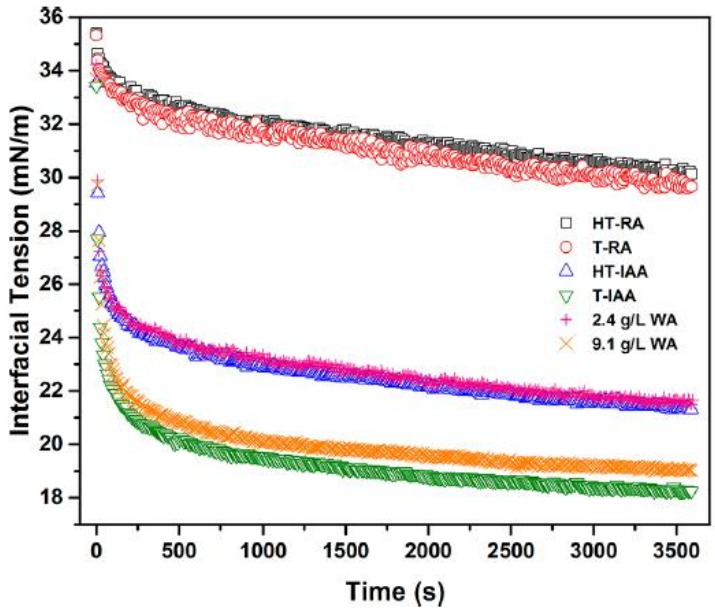

Figure 3. Dynamic interfacial tension between DI water and 0.1 g/L or equivalent (2.4 and 9.1 g/L WA-in-toluene) fractionated asphaltene-in-toluene solution.

3.2.2. Interfacial Shear Rheology. It has been shown that the viscoelasticity of interfacial asphaltene films is strongly related to the stability of W/O emulsions.30,49,50 Contacting water droplets coalesce rapidly when the film remains viscous dominant. However, as the film becomes elastic dominant, water droplets become stable and do not coalescence.30 To understand the role of interfacially active asphaltenes in stabilizing W/O emulsions, the viscoelastic moduli (G′, elastic modulus; G″, viscous modulus) of asphaltene-stabilized films were measured as a function of aging time, and the results are shown in Figure 4. For T-IAA, the G″ contribution developed at a decreasing rate while G′ remained unmeasurable until t = 7500 s. The G′ of T-IAA interfacial film continued to build up, exhibiting a viscous-to-elastic transition (G′ = G″) at t = 14 600 s, after which the film can be considered elastic dominant or “solid-like.” HT-IAA showed a similar aging profile, producing an elastic dominant interfacial film, albeit with a longer time to reach the transition (G′ = G″) as compared with T-IAA. In contrast, no measurable G′ was obtained for HT-RA and T-RA, confirming that interfacial films composed of RA subfractions remained purely viscous even after 12 h of aging. From the shear rheology measurements, it is readily evident that the IAA subfractions are the major contributor to the formation of elastic dominant asphaltene films at oil−water interfaces.

The mechanical strength of the asphaltene-stabilized interfacial film can also be inferred from the power-law dependence of G′ and G″ on the angular frequency of shear oscillations.37,51 For a viscous dominant film (G′ < G″), both G′ and G″ exhibit strong dependence on the angular frequency (ω). However, as the interface begins to strengthen (G′ > G″), the viscoelastic moduli respond as a function of ω^n with n between 0 and 1, showing weak dependence on the frequency. For a fully cross-linked system (G′ ≫ G″), G′ and G″ are entirely independent of the frequency with n = 0. The degree of cross-linking for T-IAA and HT-IAA interfacial films was evaluated by the frequency response of the asphaltene-stabilized interface after 12 h of aging. The frequency was increased from 0.001 to 0.1 Hz with a constant strain amplitude of 0.5%. As shown in Figure 5, G′ and G″ exhibit a weak dependence on angular frequency with n

smaller than 1 for both T-IAA and HT-IAA interfacial films. Furthermore, the power exponents of the T-IAA interfacial film were smaller than those of HT-IAA interfacial film, indicating that the T-IAA interfacial film is more cross-linked, supporting the higher shear elasticity measured for T-IAA interfacial film.

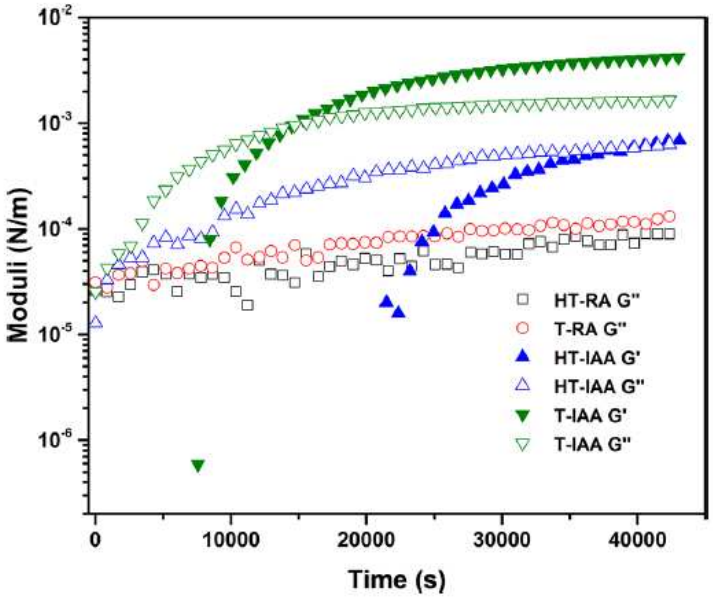

Figure 4. Time dependence of G' and G'' of interfacial films formed by asphaltene subfractions at toluene−water interfaces.

3.2.3. Crumpling Ratio. The formation of solid-like asphaltene interfacial films was further confirmed by the crumpling ratio measurement. Due to the irreversible adsorption of asphaltenes and formation of rigid asphaltene films that resist in-plane shear, asphaltene-stabilized interfaces buckle during droplet volume reduction when the compressive yield of the film is surpassed.34,52,53 The crumpling ratios of oil droplets (0.1 g/L fractionated asphaltene-in-toluene solutions) aged in DI water for 1 h were measured, and the results are summarized in Table 3. Unlike interfacial shear rheology where the interfacial area remains constant, the crumpling ratio measurement relies on reducing the interfacial area, with more rigid films exhibiting a higher crumpling ratio. The highest crumpling ratio was observed for T-IAA (0.58), followed by HT-IAA (0.38). This result is consistent with the interfacial shear rheology data which show that the T-IAA subfraction contains more interfacially active asphaltenes. These asphaltenes interact to form rigid films at oil−water interfaces. Interestingly, the HT-RA (0.24) and T-RA (0.25) subfractions resulted in a measurable crumpling ratio, even though the corresponding interfacial shear rheology confirmed a purely viscous film after 12 h of aging. The measurable crumpling ratios suggest that the RA subfractions contain a number of IAA molecules which may have not been completely removed during the fractionation due to the limited interfacial area at the given water-to-oil ratio. The presence of a small fraction of IAA in the RA subfractions is also evident by the slight reduction in the oil−water interfacial tension (Figure 3).

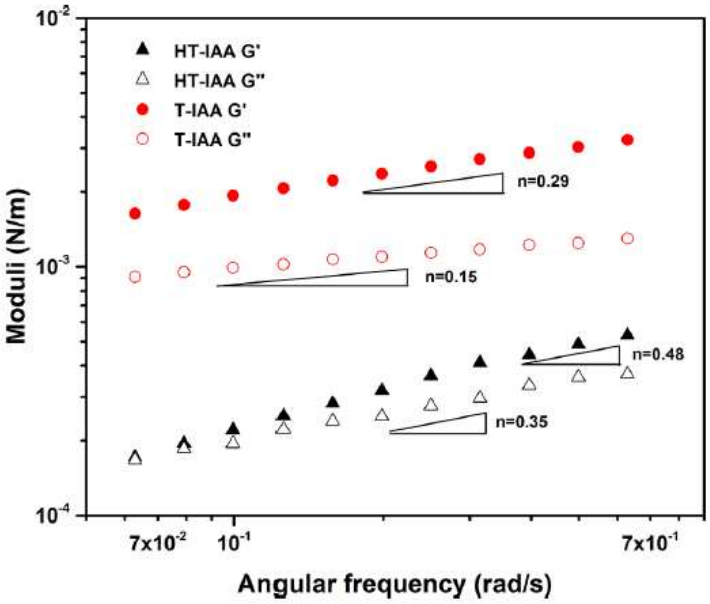

Figure 5. Frequency dependence of G' and G'' of interfacial films formed by HT-IAA and T-IAA at toluene–water interfaces.

Table 3. Crumpling Ratios of Oil Droplets (0.1 g/L Fractionated Asphaltene-in-Toluene Solutions) Aged for 1 h in DI Water

asphaltene subfraction	crumpling ratio
HT-RA	0.24
T-RA	0.25
HT-IAA	0.38
T-IAA	0.58

3.3. Emulsion Stability by Bottle Test. The emulsion stabilizing potential of different asphaltene subfractions was studied by the conventional bottle test method, wherein 10 mL of 0.1 g/L fractionated asphaltene-in-toluene solutions and 1 mL of DI water were homogenized at 30 000 rpm for 5 min. The stability of W/O emulsions against coalescence can be qualitatively evaluated based on the size distribution of water droplets, with smaller water droplets indicating reduced droplet−droplet coalescence and more stable emulsions. The settled water droplets were collected at a depth of 1 cm above the base of the sample vial, and the droplet size distribution was determined from microscopic images (analyzing 100 water droplets using ImageJ). Immediately following emulsification, the initial 50% passing size (D_{50}) was found to be similar for all emulsions, with slight variability in the narrow size range of 14−17 μm. With aging, droplets began to settle and coalesce in the densely packed bed at the bottom of the sample vial. Figure 6 shows the size distribution of water droplets 1 h after emulsification. The majority of water droplets stabilized by TIAA were in the size range of 20−40 μm, in contrast to 40−50 μm for droplets stabilized by HT-IAA. Differences in the droplet size distributions confirm that T-IAA-stabilized water droplets were more resistant to coalescence than those stabilized by HT-IAA. Moreover, much larger water droplets were observed in emulsions prepared using HT-RA and T-RA, with the droplet size distribution in the range of 60−70 μm and 50−70 μm, respectively. Free water dropout was observed only for the emulsions prepared using HT-RA and T-RA 12 h after emulsification. Therefore, W/O emulsions prepared using RA subfractions were significantly less stable against coalescence than those prepared using IAA subfractions, underlining the enhanced stabilizing potential of IAA.

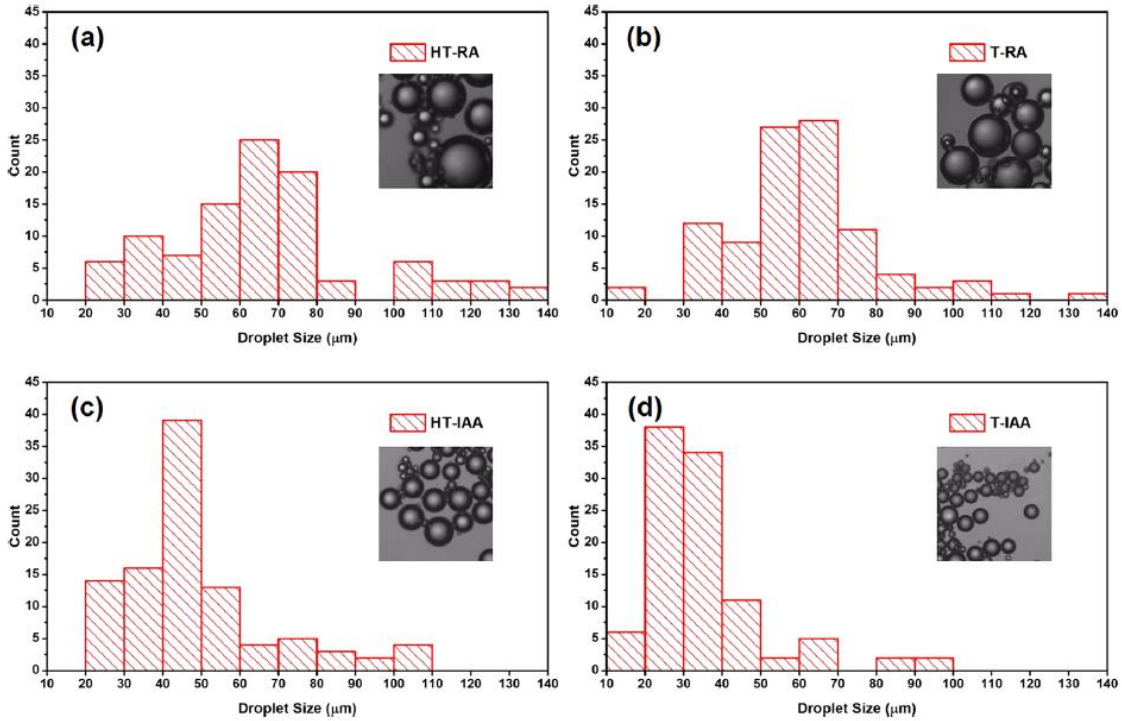

Figure 6. Size distribution of settled water droplets from W/O emulsions stabilized by (a) HT-RA, (b) T-RA, (c) HT-IAA, and (d) T-IAA, 1 h after emulsification. Inset: Microscopic images of water droplets collected at a depth of 1 cm above the vial base.

The remaining asphaltene concentration in the supernatant 1 h after emulsification was measured by UV−Vis spectroscopy. The concentration of asphaltenes in the oil phase equaled 0.035 g/L for HT-IAA and 0.005 g/L for T-IAA, confirming that 65% of HT-IAA and 95% of T-IAA were adsorbed at the oil−water interface during emulsification. However, 84% of HT-RA and 82% of T-RA remained in the oil phase, clearly demonstrating that the presence of a small amount of IAA molecules in RA subfractions was not sufficient to stabilize W/O emulsions.

W/O emulsions prepared using T-IAA and HT-IAA can be considered stable since free water dropout was not observed after 12 h aging. Hence, the asphaltene "blocking" coverage to prevent water droplet coalescence can be estimated as follows. Based on the definition of droplet Sauter mean diameter,[54,55] d32 is given by

$$d_{32} = \frac{\sum n_i d_i^3}{\sum n_i d_i^2} \quad (1)$$

where ni is the number frequency of water droplets of diameter di. d32 for HT-IAA and T-IAA was determined to be 62.8 and 50.1 μm, respectively. Assuming that asphaltenes stabilize W/O emulsions by forming a dense monolayer of asphaltene molecules,[54−57] the surface mass coverage (Γasp) of asphaltenes can be approximated by

$$\Gamma_{asp} = \frac{M'_{asp}}{A_w} \quad (2)$$

where M'asp is the mass of asphaltenes adsorbed at the oil−water interface, and the total interfacial area (Aw) of the emulsion can be obtained from the Sauter mean diameter and the total volume of emulsified water (Vw)

$$A_w = \frac{6V_w}{d_{32}} \quad (3)$$

By combining eqs 2 and 3, Γasp can be expressed as

$$\Gamma_{asp} = \frac{M'_{asp} d_{32}}{6V_w} = \frac{(1-\alpha_w)(C^i_{asp} - C''_{asp})d_{32}}{6\alpha_w} \quad (4)$$

where αw is the volume fraction of water, C'asp is the initial concentration of asphaltenes in the oil phase before emulsification, and C"asp is the concentration of asphaltenes remaining in the oil phase 1 h after emulsification. Previous research studying WA showed a critical blocking coverage of ~3.5 mg/m2, which was independent of the emulsification method.[54,55] Based on the calculation sequence, the value of Γasp value for HT-IAA and T-IAA was found to be subfractions equals 6.8 and 7.9 mg/m2, respectively, which is higher than the value of 3.5 mg/m2 reported for WA.

4. DISCUSSION

Four asphaltene subfractions were prepared using the E-SARA method.[25,27] The influence of solvent aromaticity on interfacial activity of asphaltenes and subsequent effect on the physicochemical properties of IAA subfractions were determined. Table 4 compares the physicochemical properties of the four asphaltene subfractions: T-IAA, HT-IAA, T-RA, and HTRA.

The amount of IAA was significantly influenced by the solvent aromaticity, with more IAA being recovered when the emulsion was prepared using heptol. Since the solubility of asphaltenes is reduced in less aromatic solvents,[28] asphaltenes partition more favorably at the oil−water interface from heptol than from toluene solutions,[58] thus contributing to the higher yield of HT-IAA than that of T-IAA. In spite of a similar H/C ratio and nitrogen content for all asphaltene subfractions, the elemental analysis highlighted substantial differences in oxygen content. The oxygen content of T-IAA was 1.5 times that of HT-IAA, and 3 times that of T-RA and HT-RA. As revealed by FTIR and XPS analysis, the high oxygen content of IAA subfractions manifested through the presence of sulfoxide groups, with the sulfoxide content being a single identifier for IAA subfractions.[38,59,60] The polar oxygenated sulfur- and carbon-containing groups were found to enhance the interfacial adsorption of asphaltenes mainly through hydrogen bonding,[39,61] although the decreased solvent aromaticity also promoted interfacial adsorption, as highlighted by the lower amount of oxygen and sulfoxide groups in HT-IAA as compared with T-IAA. However, the reduced solvency of asphaltenes in heptol encourages lesser interfacially active asphaltenes to partition at the oil−water interface. Therefore, when two asphaltene subfractions were redissolved in toluene at the same concentration (0.1 g/L), the HT-IAA subfraction contains comparatively less IAA than the T-IAA subfraction and was shown to be less interfacially active. Both IAA subfractions are considerably more interfacially active than the two RA subfractions. The IAA subfractions packed densely at the toluene−water interface (Γasp = 7.9 mg/m2 for T-IAA; 6.8 mg/m2 for HT-IAA), with surface coverage being approximately twice the previously reported value for WA.[54,55] The surface coverage of asphaltenes at the oil−water interface is likely to be a contributing factor to the observed differences between the four asphaltene subfractions, providing a justification for the lowest interfacial tension and highest interfacial film rigidity formed by the T-IAA subfraction.

Table 4. Comparison of Physicochemical Properties of Four Asphaltene Subfractions

	T-IAA	HT-IAA	T-RA	HT-RA
yield (wt %)	1.1 ± 0.3	4.2 ± 0.3	98.9 ± 0.3	95.8 ± 0.3
O (wt %)	5.62	3.71	1.37	1.34
S (wt %)	9.78	9.72	8.76	8.74
sulfoxide (%)[a]	22.43	19.24	n/a	n/a
IFT (mN/m;[b] t = 1 h)	18.27	21.33	29.66	30.14
G'/G''[b] (t = 12 h)	2.51	1.07	n/a	n/a
D_{50} (μm;[b] t = 1 h)	35.6	43.5	58.2	64.2
Γ_{asp} (mg/m^2)[b]	7.9	6.8	n/a	n/a

[a]The sulfoxide percent was determined by the peak area ratio of sulfoxide from the XPS S 2p band of each asphaltene subfraction. [b]The oil phases were 0.1 g/L fractionated asphaltene-in-toluene solutions with DI water as the water phase.

5. CONCLUSION

Asphaltene fractionation by E-SARA according to their adsorption characteristics at oil−water interfaces was studied in solvents of different aromaticities: toluene and heptol. The research further supports the notion that not all asphaltene molecules contribute equally to stabilization of W/O petroleum emulsions. Despite the small proportion of IAA subfractions in WA, the IAA subfractions were recognized as the predominant contributor to stabilization of W/O emulsions rather than the more abundant RA subfractions. The aromaticity of solvents (toluene vs heptol) had an

insignificant impact on the elemental compositions of RA subfractions. However, larger amounts of sulfur and oxygen were observed in T-IAA than in HT-IAA.

Even though both IAA (T-IAA and HT-IAA) subfractions were considered to be irreversibly adsorbed at oil−water interfaces, differences in their elemental compositions led to differences in asphaltene interfacial activity and properties of their interfacial films. The T-IAA subfraction formed a densely packed network that was more elastic and resistant to drop−drop coalescence than the system prepared using HT-IAA. As indicated by FTIR and XPS analysis, the oxygenated groups, in particular sulfoxides, play a critical role in the interfacial activity of asphaltenes. T-IAA contained the highest content of sulfoxides, followed by HT-IAA, then T-RA and HT-RA. The current research further elucidates that sulfoxide is the key functional group responsible for asphaltene adsorption at oil−water interfaces and subsequently the stabilization of W/O emulsions. Such knowledge is necessary to design smarter chemicals and processing strategies to mitigate asphaltene related issues (emulsion stabilization, deposition, etc.) which begin when the interfacially active asphaltenes first adsorb or deposit at the liquid−liquid or solid−liquid interfaces.

Corresponding Author
*E-mail: zhenghe.xu@ualberta.ca.
ORCID
David Harbottle: 0000-0002-0169-517X
Zhenghe Xu: 0000-0001-8118-1920
Notes
The authors declare no competing financial interest.

ACKNOWLEDGMENTS
This research was conducted under the auspices of the Natural Sciences and Engineering Research Council (NSERC)-Industrial Research Chair (IRC) Program in Oil Sands Engineering. The partial support from Alberta Innovates Energy and Environmental Solutions and from National Natural Science Foundation of China (Grant 21333005) is also greatly appreciated.

REFERENCES
(1) Sjoblom, J.; Aske, N.; Auflem, I. H.; Brandal, Ø.; Havre, T. E.; Sæther, Ø.; Westvik, A.; Johnsen, E. E.; Kallevik, H. Adv. Colloid Interface Sci. 2003, 100, 399−473.
(2) Kilpatrick, P. K. Energy Fuels 2012, 26, 4017−4026.
(3) Wong, S. F.; Lim, J. S.; Dol, S. S. J. Pet. Sci. Eng. 2015, 135, 498−504.
(4) Harbottle, D.; Liang, C.; El-thaher, N.; Liu, Q.; Masliyah, J.; Xu, Z. Particle-stabilized emulsions in heavy oil processing. In Particle Stabilized Emulsions and Colloids: Formation and Application; Ngai, T., Bon, S. A. F., Eds.; The Royal Society of Chemistry: London, UK, 2015.
(5) Akbarzadeh, K.; Hammami, A.; Kharrat, A.; Zhang, D.; Allenson, S.; Creek, J.; Kabir, S.; Jamaluddin, A. J.; Marshall, A. G.; Rodgers, R. P.; Mullins, O. C.; Solbakken, T. Oilfield. Rev. 2007, 19, 22−43.
(6) Mullins, O. C. Annu. Rev. Anal. Chem. 2011, 4, 393−418.
(7) Langevin, D.; Argillier, J.-F. Adv. Colloid Interface Sci. 2016, 233, 83−93.
(8) McLean, J. D.; Kilpatrick, P. K. J. Colloid Interface Sci. 1997, 196, 23−34.
(9) Sheu, E. Y. Energy Fuels 2002, 16, 74−82.
(10) He, L.; Lin, F.; Li, X.; Sui, H.; Xu, Z. Chem. Soc. Rev. 2015, 44, 5446−5494.
(11) Czarnecki, J.; Tchoukov, P.; Dabros, T. Energy Fuels 2012, 26, 5782−5786.
(12) Xu, Y.; Dabros, T.; Hamza, H.; Shefantook, W. Pet. Sci. Technol. 1999, 17, 1051−1070.
(13) Czarnecki, J.; Tchoukov, P.; Dabros, T.; Xu, Z. Can. J. Chem. Eng. 2013, 91, 1365−1371.
(14) Stanford, L. A.; Rodgers, R. P.; Marshall, A. G.; Czarnecki, J.; Wu, X. A. Energy Fuels 2007, 21, 963−972.
(15) Wu, X. Energy Fuels 2003, 17, 179−190.
(16) Adams, J. J. Energy Fuels 2014, 28, 2831−2856.
(17) Wattana, P.; Fogler, H. S.; Yen, A.; Carmen Garcia, M. D.; Carbognani, L. Energy Fuels 2005, 19, 101−110.
(18) Rogel, E.; Miao, T.; Vien, J.; Roye, M. Fuel 2015, 147, 155−160.
(19) Tu, Y.; Woods, J.; Kung, J.; McCracken, T.; Kotlyar, L.; Sparks, B.; Dong, M. Clay Sci. 2006, 12, 183−187.
(20) Tu, Y.; Kung, J.; McCracken, T.; Kotlyar, L.; Kingston, D.; Sparks, B. Clay Sci. 2006, 12, 194−198.
(21) Tu, Y.; Woods, J.; McCracken, T.; Kotlyar, L.; Sparks, B.; Chung, K. Clay Sci. 2006, 12, 188−193.
(22) Spiecker, P. M.; Gawrys, K. L.; Kilpatrick, P. K. J. Colloid Interface Sci. 2003, 267, 178−193.
(23) Östlund, J.-A.; Nydén, M.; Fogler, H. S.; Holmberg, K. Colloids Surf., A 2004, 234, 95−102.
(24) Kharrat, A. M. Energy Fuels 2009, 23, 828−834.
(25) Qiao, P.; Harbottle, D.; Tchoukov, P.; Masliyah, J. H.; Sjoblom, J.; Liu, Q.; Xu, Z. Energy Fuels 2017, 31, 3330−3337.
(26) Subramanian, S.; Simon, S.; Gao, B.; Sjöblom, J. Colloids Surf., A 2016, 495, 136−148.

(27) Yang, F.; Tchoukov, P.; Pensini, E.; Dabros, T.; Czarnecki, J.; Masliyah, J.; Xu, Z. Energy Fuels 2014, 28, 6897−6904.
(28) Tchoukov, P.; Czarnecki, J.; Dabros, T. Colloids Surf., A 2010, 372, 15−21.
(29) Tchoukov, P.; Yang, F.; Xu, Z.; Dabros, T.; Czarnecki, J.; Sjöblom, J. Langmuir 2014, 30, 3024−3033.
(30) Harbottle, D.; Chen, Q.; Moorthy, K.; Wang, L.; Xu, S.; Liu, Q.; Sjoblom, J.; Xu, Z. Langmuir 2014, 30, 6730−6738.
(31) Eley, D. D.; Hey, M. J.; Symonds, J. D. Colloids Surf. 1988, 32, 87−101.
(32) Wang, S.; Liu, J.; Zhang, L.; Masliyah, J.; Xu, Z. Langmuir 2010, 26, 183−190.
(33) Natarajan, A.; Xie, J.; Wang, S.; Liu, Q.; Masliyah, J.; Zeng, H.; Xu, Z. J. Phys. Chem. C 2011, 115, 16043−16051.
(34) Zhang, L.; Shi, C.; Lu, Q.; Liu, Q.; Zeng, H. Langmuir 2016, 32, 4886−4895.
(35) Mannistu, K. D.; Yarranton, H. W.; Masliyah, J. H. Energy Fuels 1997, 11, 615−622.
(36) Vilas Bôas FáVero, C.; Maqbool, T.; Hoepfner, M.; Haji-Akbari, N.; Fogler, H. S. Adv. Colloid Interface Sci. 2016, 244, 267−280.
(37) Bi, J.; Yang, F.; Harbottle, D.; Pensini, E.; Tchoukov, P.; Simon, S.; Sjöblom, J.; Dabros, T.; Czarnecki, J.; Liu, Q.; Xu, Z. Langmuir 015, 31, 10382−10391.
(38) Stanford, L. A.; Rodgers, R. P.; Marshall, A. G.; Czarnecki, J.; Wu, X. A.; Taylor, S. Energy Fuels 2007, 21, 973−981.
(39) Yang, F.; Tchoukov, P.; Dettman, H.; Teklebrhan, R. B.; Liu, L.; Dabros, T.; Czarnecki, J.; Masliyah, J.; Xu, Z. Energy Fuels 2015, 29, 4783−4794.
(40) Rudrake, A.; Karan, K.; Horton, J. H. J. Colloid Interface Sci. 2009, 332, 22−31.
(41) Abdallah, W. A.; Taylor, S. D. J. Phys. Chem. C 2008, 112, 18963−18972.
(42) Abudu, A.; Goual, L. Energy Fuels 2009, 23, 1237−1248.
(43) Siskin, M.; Kelemen, S. R.; Eppig, C. P.; Brown, L. D.; Afeworki, M. Energy Fuels 2006, 20, 1227−1234.
(44) Kozłowski, M. Fuel 2004, 83, 259−265.
(45) Liu, F.; Li, W.; Chen, H.; Li, B. Fuel 2007, 86, 360−366.
(46) Abdallah, W. A.; Taylor, S. D. Nucl. Instrum. Methods Phys. Res., Sect. B 2007, 258, 213−217.
(47) Jeribi, M.; Almir-Assad, B.; Langevin, D.; Hénaut, I.; Argillier, J. F. J. Colloid Interface Sci. 2002, 256, 268−272.
(48) Pauchard, V.; Rane, J. P.; Zarkar, S.; Couzis, A.; Banerjee, S. Langmuir 2014, 30, 8381−8390.
(49) Spiecker, P. M.; Kilpatrick, P. K. Langmuir 2004, 20, 4022−4032.
(50) Pensini, E.; Harbottle, D.; Yang, F.; Tchoukov, P.; Li, Z.; Kailey, I.; Behles, J.; Masliyah, J.; Xu, Z. Energy Fuels 2014, 28, 6760−6771.
(51) Verruto, V. J.; Le, R. K.; Kilpatrick, P. K. J. Phys. Chem. B 2009, 113, 13788−13799.
(52) Gao, S.; Moran, K.; Xu, Z.; Masliyah, J. Energy Fuels 2009, 23, 2606−2612.
(53) Yeung, A.; Dabros, T.; Masliyah, J.; Czarnecki, J. Colloids Surf., A 2000, 174, 169−181.
(54) Yarranton, H. W.; Hussein, H.; Masliyah, J. H. J. Colloid Interface Sci. 2000, 228, 52−63.
(55) Pauchard, V.; Roy, T. Colloids Surf., A 2014, 443, 410−417.
(56) Sztukowski, D. M.; Jafari, M.; Alboudwarej, H.; Yarranton, H. W. J. Colloid Interface Sci. 2003, 265, 179−186.
(57) Rane, J. P.; Zarkar, S.; Pauchard, V.; Mullins, O. C.; Christie, D.; Andrews, A. B.; Pomerantz, A. E.; Banerjee, S. Energy Fuels 2015, 29, 3584−3590.
(58) Kiran, S. K.; Acosta, E. J.; Moran, K. Energy Fuels 2009, 23, 3139−3149.
(59) Muller, H.; Pauchard, V. O.; Hajji, A. A. Energy Fuels 2009, 23, 1280−1288.
(60) Jarvis, J. M.; Robbins, W. K.; Corilo, Y. E.; Rodgers, R. P. Energy Fuels 2015, 29, 7058−7064.
(61) Teklebrhan, R. B.; Ge, L.; Bhattacharjee, S.; Xu, Z.; Sjöblom, J. J. Phys. Chem. B 2014, 118, 1040−1051.